Supplement of

Driving factors of aerosol acidity: a new hierarchical quantitative analysis framework and its application in Changzhou, China

Xiaolin Duan[1,#], Guangjie Zheng[1,#,*], Chuchu Chen[1,*], Qiang Zhang[2,*], Kebin He[1]

[1] State Key Joint Laboratory of Environmental Simulation and Pollution Control, School of Environment, Tsinghua University, Beijing 100084, China

[2] Ministry of Education Key Laboratory for Earth System Modeling, Department of Earth System Science, Tsinghua University, Beijing, China.

[#] These authors contributed equally.

Correspondence to: G. Zheng (zgj123@mail.tsinghua.edu.cn); C. Chen (chencc3@mail.tsinghua.edu.cn); Q. Zhang (qiangzhang@tsinghua.edu.cn)

This 13-pages PDF file contains:

- Supplementary Texts S1-S2
- Figures S1-S10

Supplementary Text

S1. Detailed description of variation contribution quantification

To illustrate the one-at-a-time sensitivity analysis method, driving factor analysis of c_{ni} variations is taken for example here. The c_{ni} depends mainly on RH, temperature T and the fraction of NO_3^- in anions ($f_{NO_3^-}$) (Zheng et al., 2022a). Based on the calculation method of previous study [19] and ISORROPIA model, these influencing factors contributions to c_{ni} variations can be quantitative analyzed by Eqs.S1 as:

$$\partial c_{\mathrm{ni}}/\partial_{RH} = c_{\mathrm{ni}}\left(\mathrm{RH}, \bar{T}, \overline{f_{NO_3^-}}\right) - c_{\mathrm{ni}}\left(\overline{\mathrm{RH}}, \bar{T}, \overline{f_{NO_3^-}}\right) \quad \text{(S1a)}$$

$$\partial c_{\mathrm{ni}}/\partial_{f_{NO_3^-}} = c_{\mathrm{ni}}\left(\overline{\mathrm{RH}}, \bar{T}, f_{NO_3^-}\right) - c_{\mathrm{ni}}\left(\overline{\mathrm{RH}}, \bar{T}, \overline{f_{NO_3^-}}\right) \quad \text{(S1b)}$$

$$\partial c_{\mathrm{ni}}/\partial_{T} = \partial c_{\mathrm{ni}} - \partial c_{\mathrm{ni}}/\partial_{f_{NO_3^-}} - \partial c_{\mathrm{ni}}/\partial_{RH} \quad \text{(S1c)}$$

where $\overline{\mathrm{X}}$ and X are the average values and decomposed values of variable X, respectively, and more detailed calculations are described in SI Text S2.

S2. Detailed descriptions of quantitative analysis of each factor based on ISM and time series analysis

Here we adopted a bottom-up method to quantify the time series components of upper-level factors in the ISM model and its driving factors. That is, based on the decomposition of time series analysis, each input parameter p in ISORROPIA v2.3 is subdivided into 4 time series components. For example, temperature can be decomposed into long-term trend (T_{yr}), seasonal variations (T_{seas}), diurnal cycles (T_{day}) and residuals (T_{res}), respectively. Then, the corresponding components are used in ISORROPIA calculations to achieve the quantitative assessment of factors affecting pH at corresponding time series.

Taking factors contribution to X_{gp} seasonal variations for example, there are two parts for calculation: $\partial X_{gp}|_{seas}$ and factor x_i contribution to $\partial X_{gp}|_{seas}$ (i.e., $\partial X_{gp}/\partial x_i|_{seas}$)

(1) Calculation of X_{gp} seasonal variations $\partial X_{gp}|_{seas}$

In the seasonal variation's scenario, values of input parameter p is (Eq. S2a)

$$p = \bar{p} + p_{seas} \quad \text{(S2a)}$$

where $\bar{p}$ is the average values of p and p_{seas} is the decomposed seasonal values in time series analysis. Based on Eq. S2a, ISORROPIA v2.3 and Eq.2d in main text, $X_{gp}|_{calc}$ is obtained. Then $\partial X_{gp}|_{seas}$ is calculate as (Eq. S2b)

$$\partial X_{gp}|_{seas} = X_{gp}|_{calc} - \overline{X_{gp}} \tag{S2b}$$

where $\overline{X_{gp}}$ is obtained based on average values of input parameters.

(2) Calculation of factor contributions $\partial X_{gp}/\partial x_i|_{seas}$

With the ISM in main text, main influence factors of X_{gp} are temperature and relative abundance of alkaline to acidic substances (C_t/A_t). These factors variations contribute to $\partial X_{gp}|_{seas}$ are obtained as follows:

$$\partial X_{gp}/\partial T|_{seas} = X_{gp}\left(T_{seas} + \bar{T}, \overline{C_t/A_t}\right) - X_{gp}\left(\bar{T}, \overline{C_t/A_t}\right) \tag{S2c}$$

$$\partial X_{gp}/\partial (C_t/A_t)|_{seas} = \partial X_{gp}|_{seas} - \partial X_{gp}/\partial T|_{seas} \tag{S2d}$$

where T_{seas} is the decomposed seasonal variations of temperature. $\overline{C_t/A_t}$ is obtained based on the base-line values of input parameters. As for C_t/A_t, its contribution to $\partial X_{gp}|_{seas}$ is the differences between $\partial X_{gp}|_{seas}$ and $\partial X_{gp}/\partial T|_{seas}$(Eq. S2d), and this approach is also applicable to contribution of $PM_{2.5}$ to AWC, temperature to c_{ni} and chemical profiles to $f_{NO_3^-}$. Then quantitative contributions of middle-level influencing factors for $\partial X_{gp}|_{seas}$ are obtained. The contributions of middle-level factors to top-level influencing factors are calculated using a similar process for each time series component. Ultimately, the quantitative contributions of chemical profiles, RH, temperature and $PM_{2.5}$ concentrations to pH are obtained for each time series component as well as for the entire observation period.

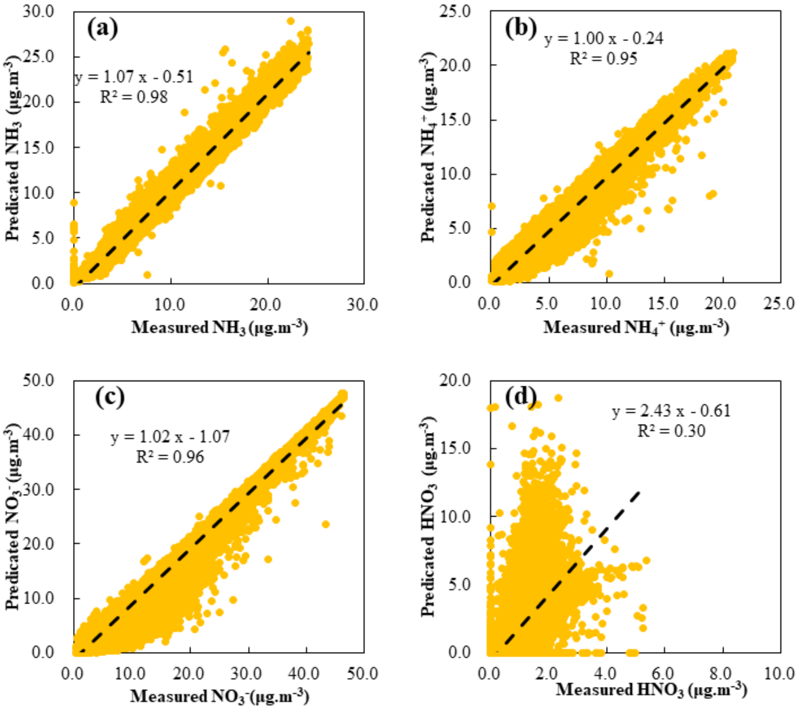

Figure S1: Comparations of predicted and measured (a) NH_3, (b) NH_4^+, (c) NO_3^-, and (d) HNO_3 concentrations in Changzhou during 2018-2023.

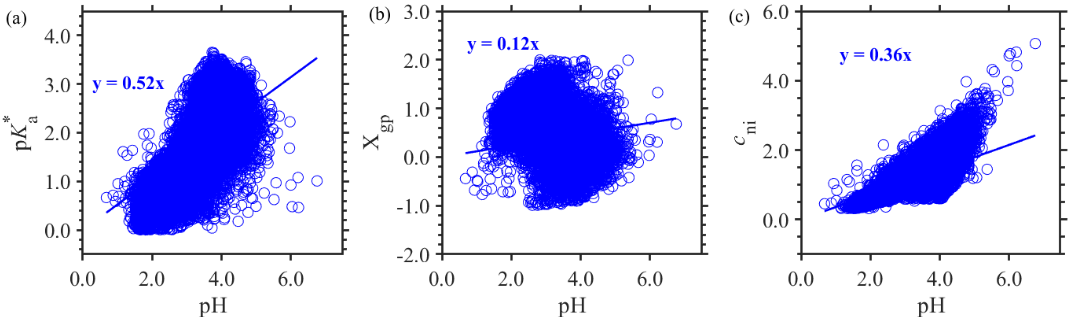

Figure S2: Top-level decomposition of pH into (a) pK_a^*, (b) X_{gp} and (c) c_{ni} during the sampling period in Changzhou.

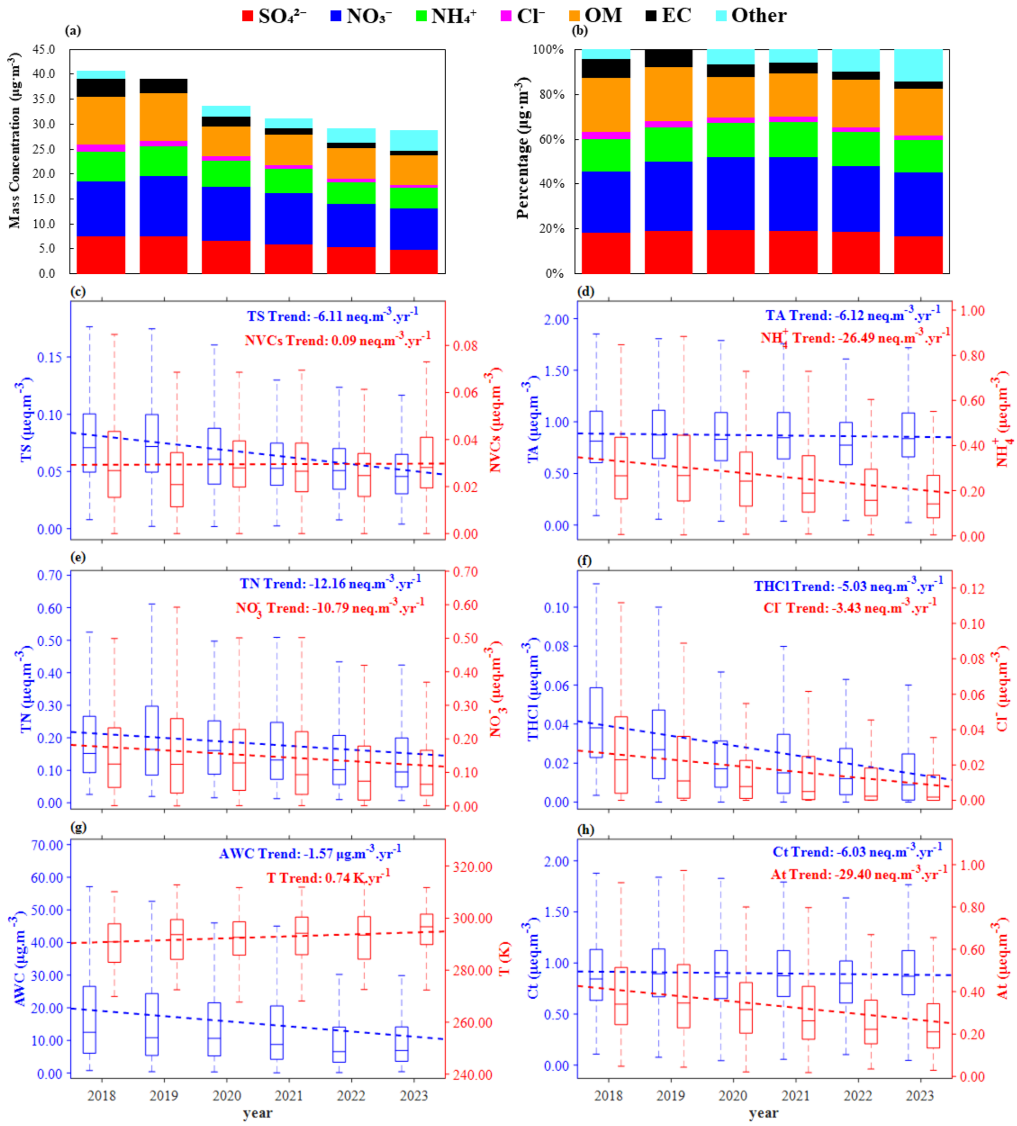

Figure S3: Long-term trends of chemical profiles and meteorology in Changzhou, China from 2018 to 2023. (a) Mean mass concentrations of chemical profiles, (b) relative percentage of chemical profiles, (c) total sulfate (TS) and non-volatile cations (NVCs), (d) total ammonia (TA) and NH_4^+, (e) total nitrate (TN) and NO_3^-, (f) total Cl^- (THCl) and Cl^-, (g) AWC and T, (h) total cations (C_t) and total anions (A_t).

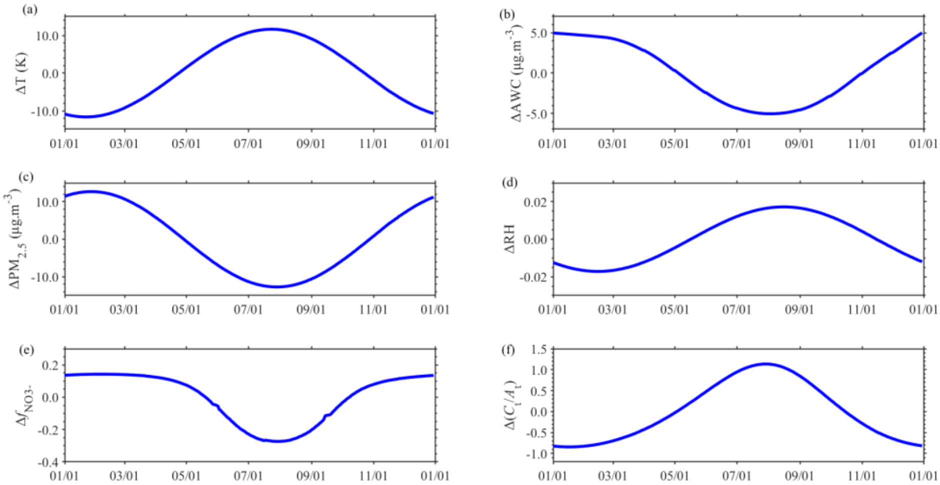

Figure S4: Seasonal variations of (a) T, (b)AWC, (c)PM$_{2.5}$, (d) RH, (e) $f_{NO_3^-}$ and (f) C_t/A_t.

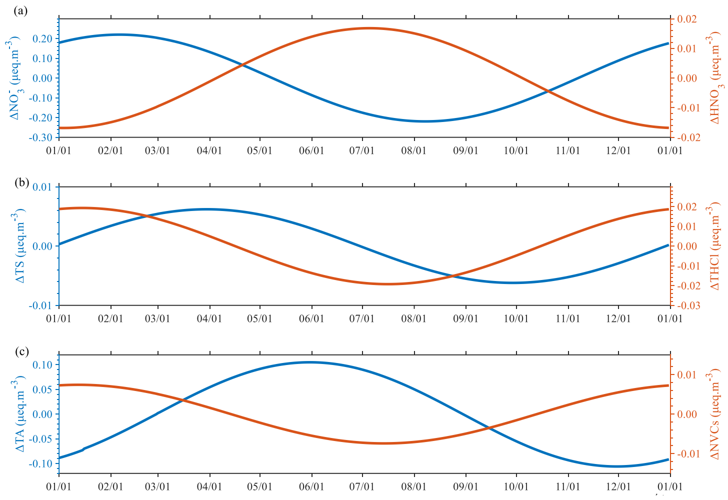

Figure S5: Seasonal variations of (a) NO_3^- and HNO_3, (b)TS and THCl, (c) TA and NVCs.

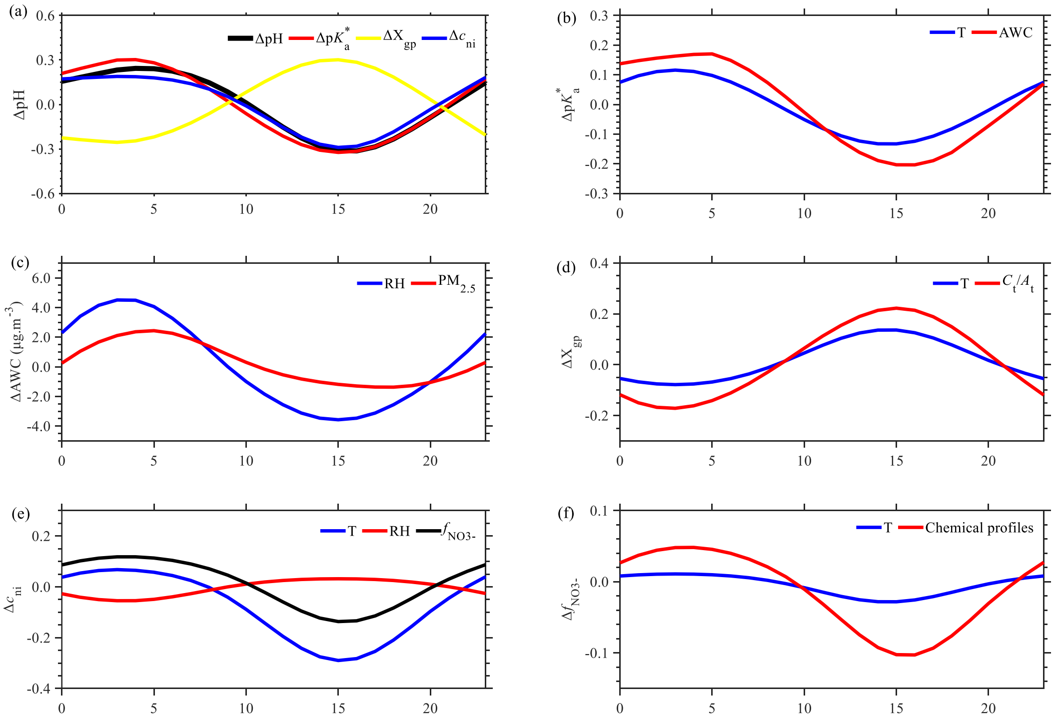

Figure S6: Influencing factors of the diurnal variations of aerosol pH. (a) The 1st level decomposition into pK_a^*, X_{gp} and c_{ni}. (b)-(f) Further investigation of the influencing factors of (b) pK_a^* due to T and AWC, (c) AWC due to RH and $PM_{2.5}$, (d)X_{gp} due to C_t/A_t and T, (e) c_{ni} due to RH, T, $\boldsymbol{f}_{NO_3^-}$, and (f) $\boldsymbol{f}_{NO_3^-}$ due to T and chemical profiles.

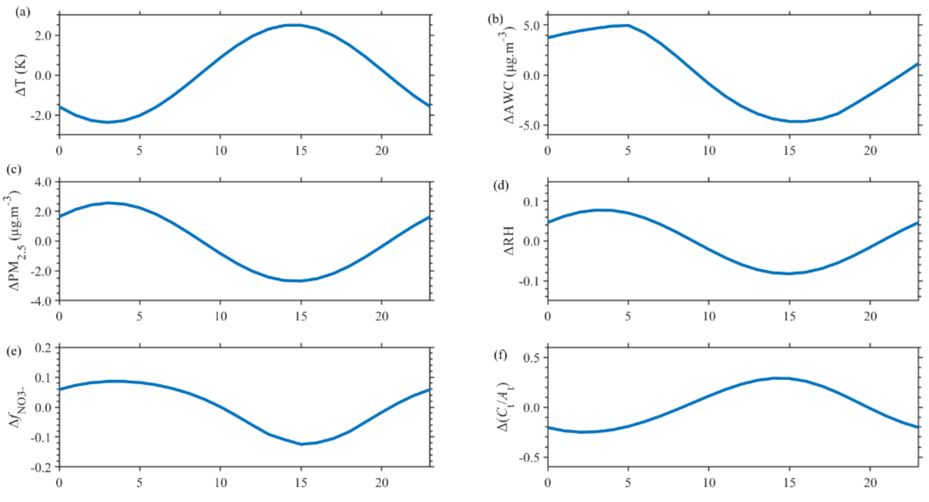

Figure S7: Diurnal cycles of (a) *T*, (b)AWC, (c)PM$_{2.5}$, (d) RH, (e) $f_{NO_3^-}$ and (f) C_t/A_t.

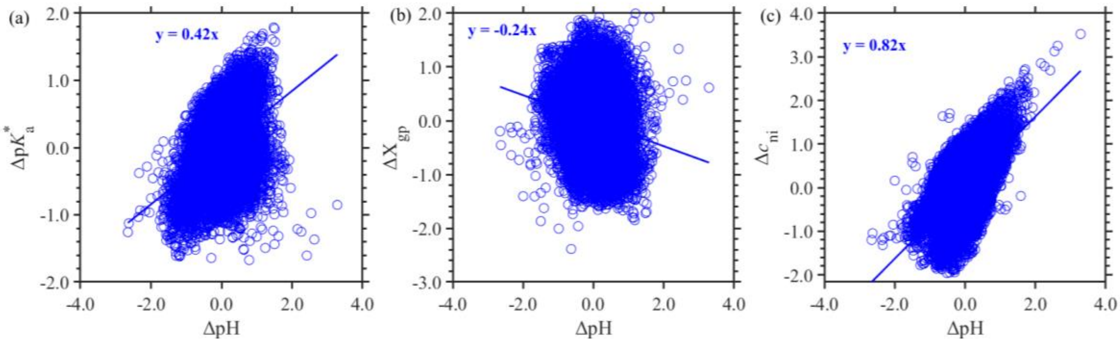

Figure S8: Top-level decomposition of random variations of pH into (a) pK_a^*, (b) X_{gp} and (c) c_{ni}.

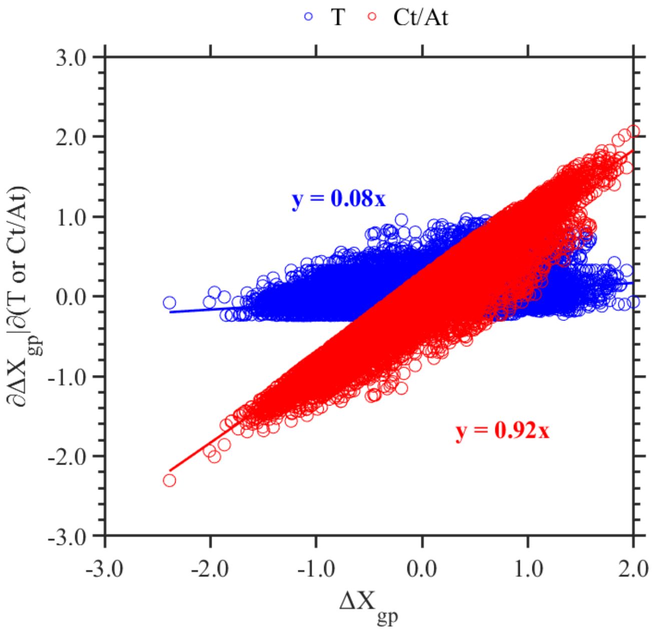

Figure S9: Random variations of X_{gp} due to T and C_t/A_t.

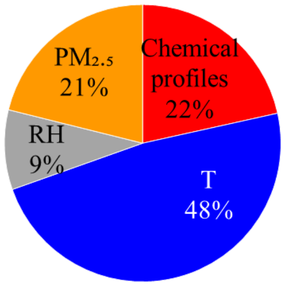

Figure S10: Overall quantitative contribution of *T*, chemical profiles, $PM_{2.5}$ and RH to aerosol pH.